Electronic Supplementary Material (ESI) for Journal of Materials Chemistry A.

Supplementary information

Alginic acid-derived mesoporous carbon (Starbon®) as template and reducing agent for the hydrothermal synthesis of mesoporous $LiMn_2O_4$ grafted by carbonaceous species

Sanghoon Kim,[a] Mario De bryne,[b] Johan G. Alauzun,[a] Nicolas Louvain,[a,c] Nicolas Brun,[a] Duncan J. Macquarrie,[b] Lorenzo Stievano,[a,c] Bruno Boury,[a] Laure Monconduit,[a,c] P. Hubert Mutin[a,*]

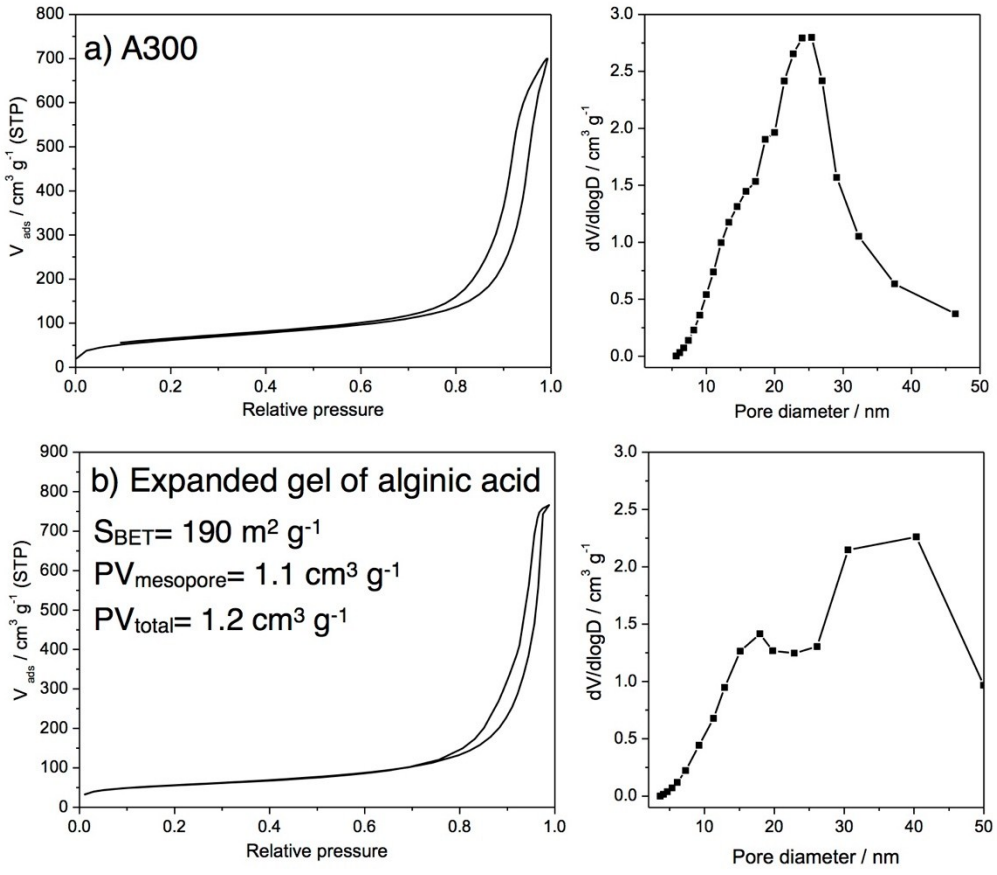

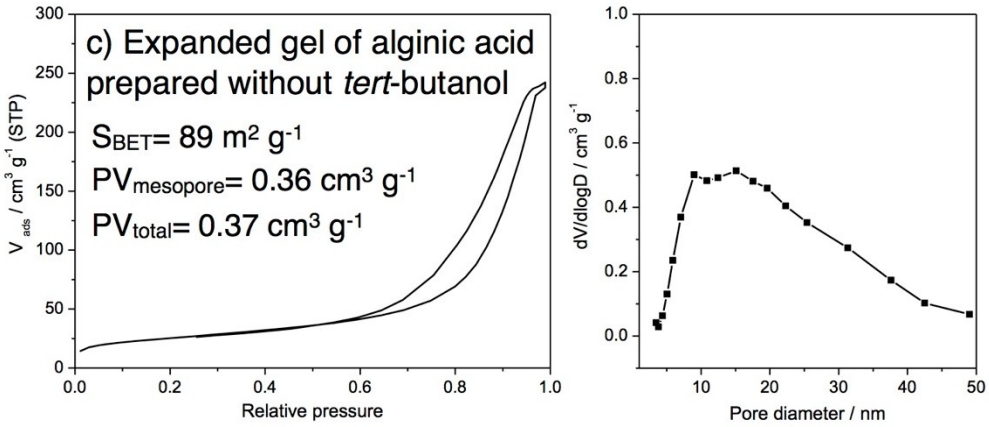

Fig. S1a. N_2 adsorption-desorption isotherm and BJH pore size distribution (desorption branch) of a) A300, b) dried expanded gel of alginic acid and c) dried expanded gel of alginic acid prepared without *tert*-butanol.

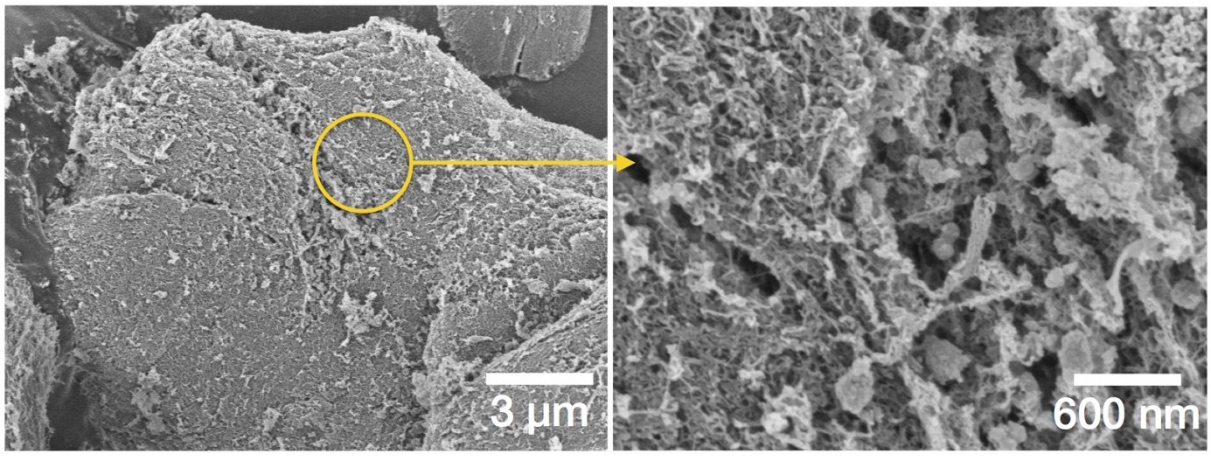

Fig. S1b. SEM images of A300.

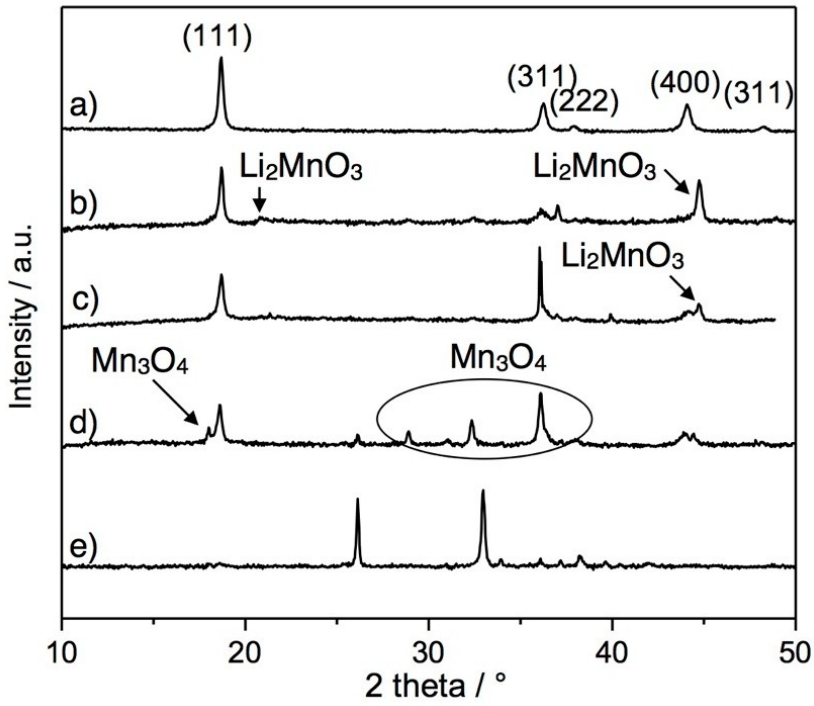

Fig. S2. Powder X-ray diffraction patterns of LMO synthesized with LiOH:$KMnO_4$ ratio of a) 2:1 (LMO-HT, as reference), b) 4:1, c) 3:1, d) 1:1 and e) 1:2.

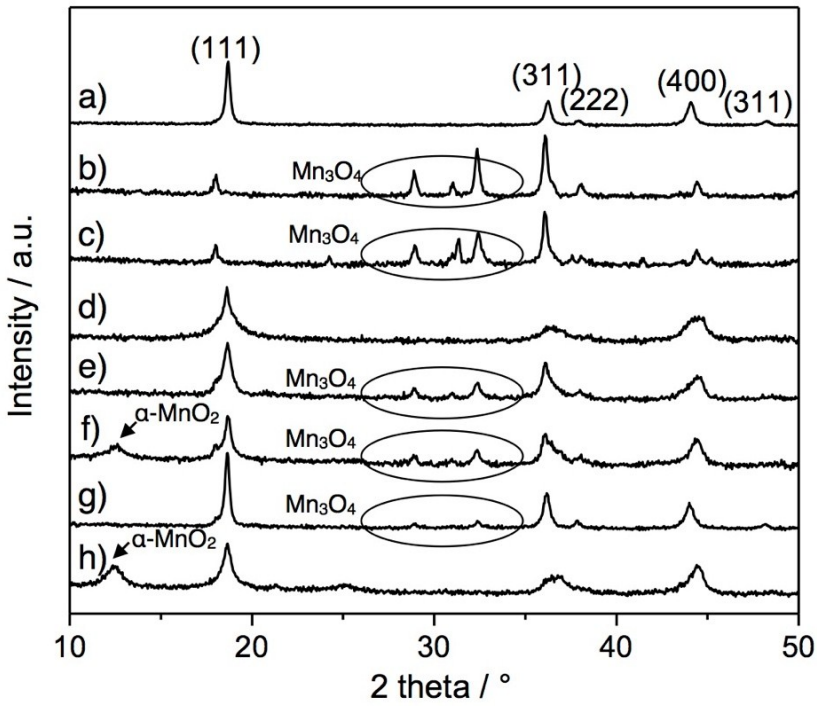

Fig. S3. Powder X-ray diffraction patterns of LMO synthesized with a 2:1 LiOH:$KMnO_4$ ratio using various amounts of A300 or different carbon materials: a) 100 mg A300 (LMO-HT); b) 50 mg of A300; c) 150 mg of A300; d) 50 mg of alginic acid, e) 50 mg of A450, f) 50 mg of A800, g) f) 50 mg of S300; h) 50 mg of Super P. A450 and A800 stand for expanded alginic acid

carbonized at 450 °C and 800 °C, respectively, S300 stands for expanded starch carbonized at 300 °C.

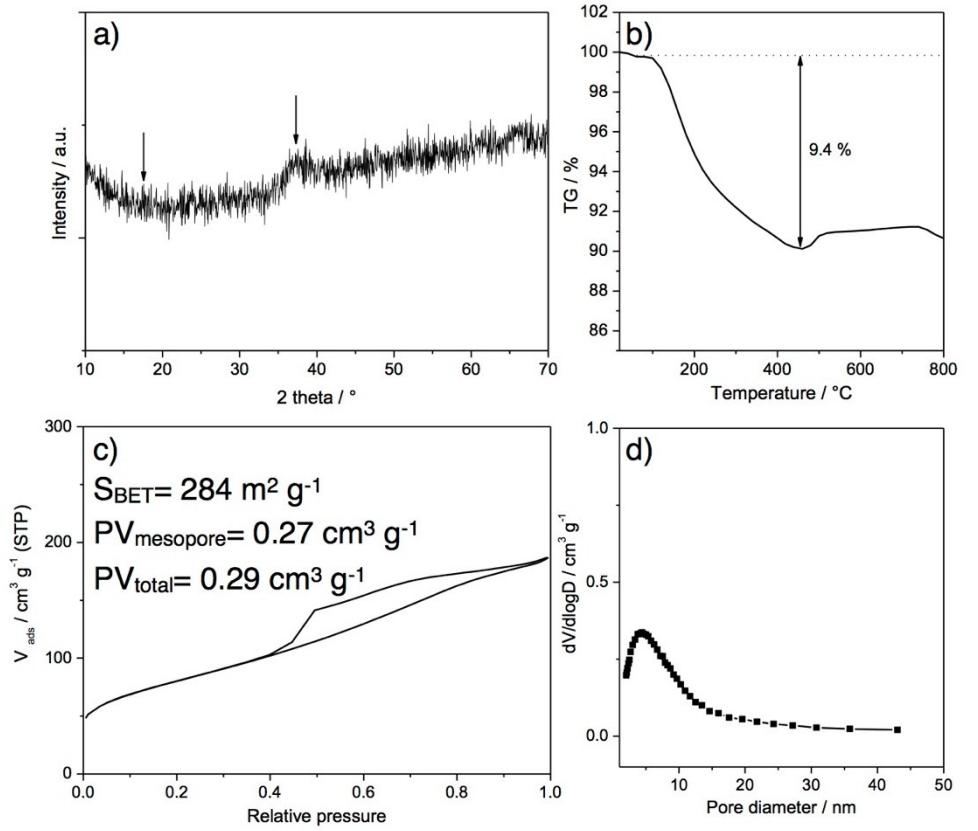

Fig. S4. Characterization of the intermediate product obtained by reaction of $KMnO_4$ with A300: a) Powder X-ray diffraction patterns showing the formation of a poorly crystalline manganese oxide phase; b) TGA in air indicating the presence of approx. 9 wt% residual A300; c) N_2 adsorption-desorption isotherm and d) BJH pore size distribution, indicating the mesoporous character of this intermediate manganese oxide/carbon composite material.

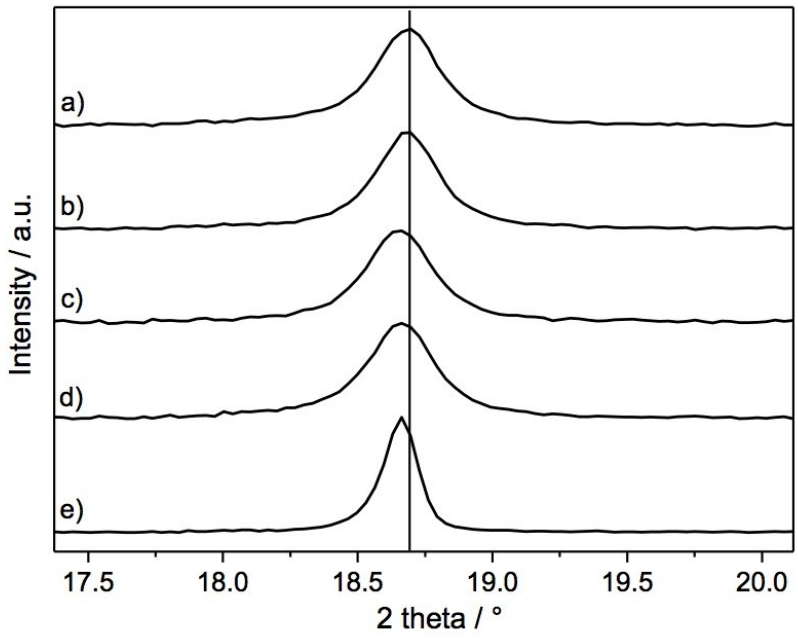

Fig. S5. Zoomed image of XRD powder X-ray diffraction patterns of a) LMO-HT, b) LMO-350, c) LMO-500, d) LMO-700 and e) LMO-Comm.

	LMO-HT	LMO-350	LMO-500	LMO-700	LMO-Comm
Lattice parameter, *a* (Å)	8.220	8.224	8.227	8.227	8.228

Table S1. Lattice parameter calculated for LMO materials of this study.

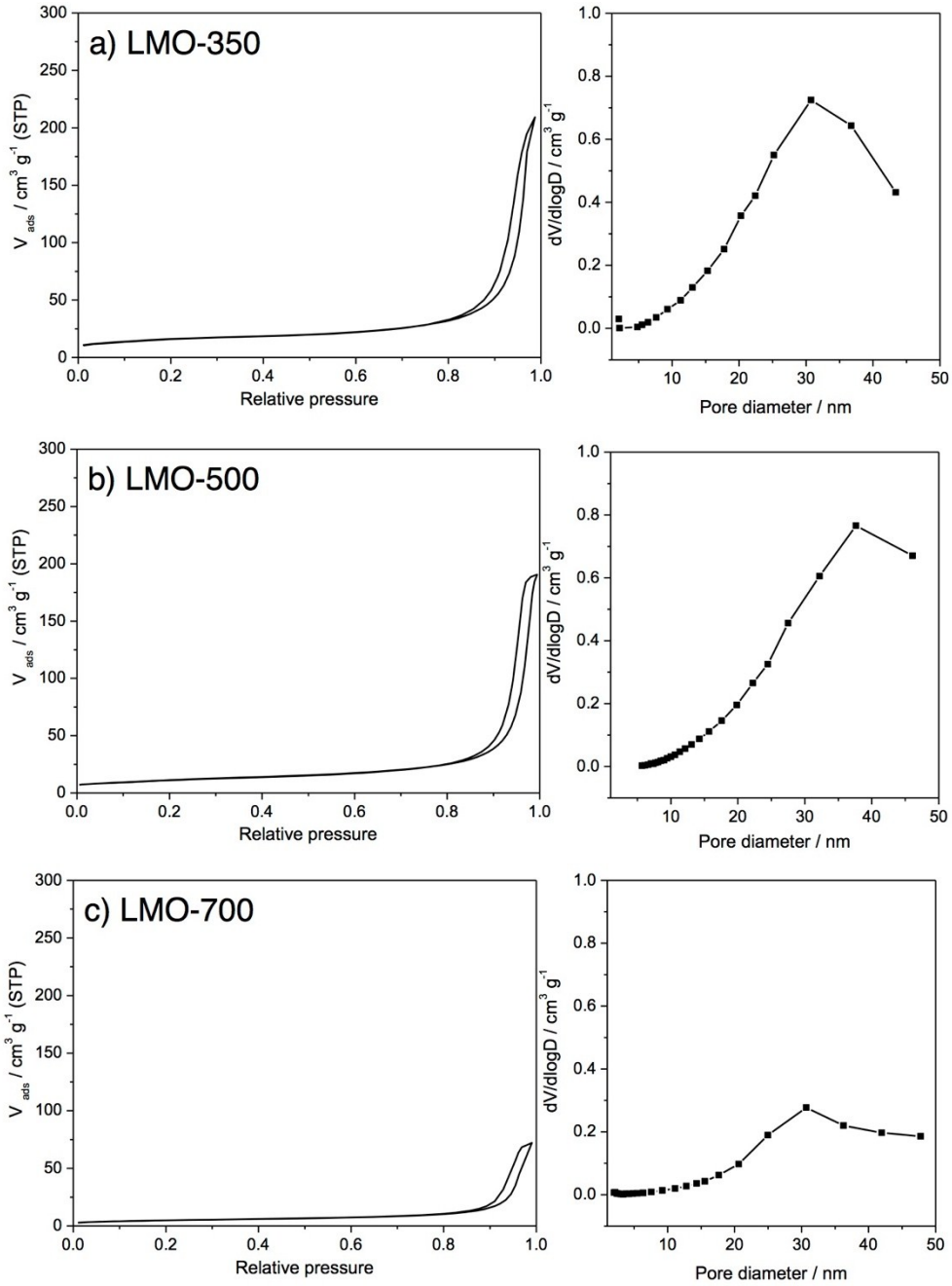

Fig. S6. N_2 adsorption-desorption isotherm and BJH pore size distribution (desorption branch) of a) LMO-350, b) LMO-500 and c) LMO-700

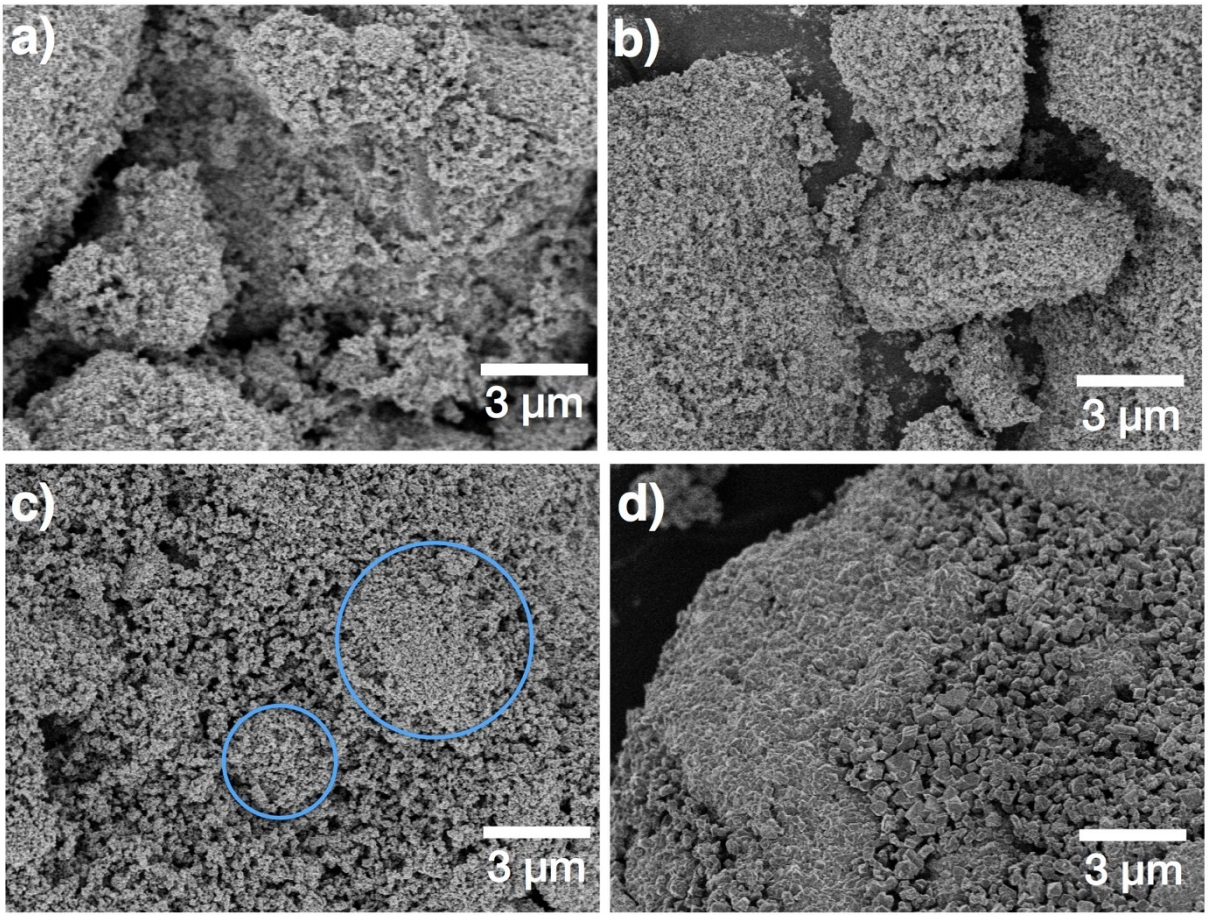

Fig. S7. Additional SEM images of a) LMO-350, b) LMO-500, c) LMO-700 (collapse of porous network can be seen in circled zones) and d) LMO-Comm.

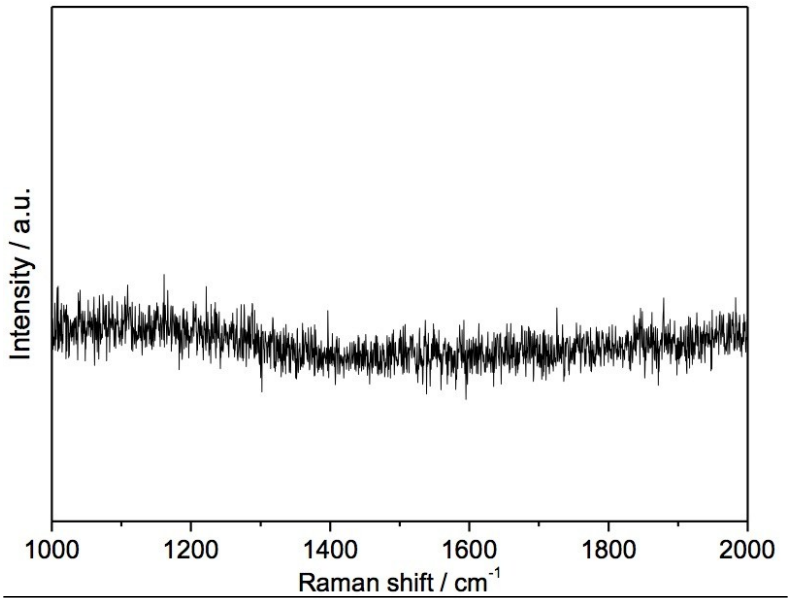

Fig. S8. Raman spectrum of LMO-HT: D or G-band were not observed, confirming the absence of graphitic structures.

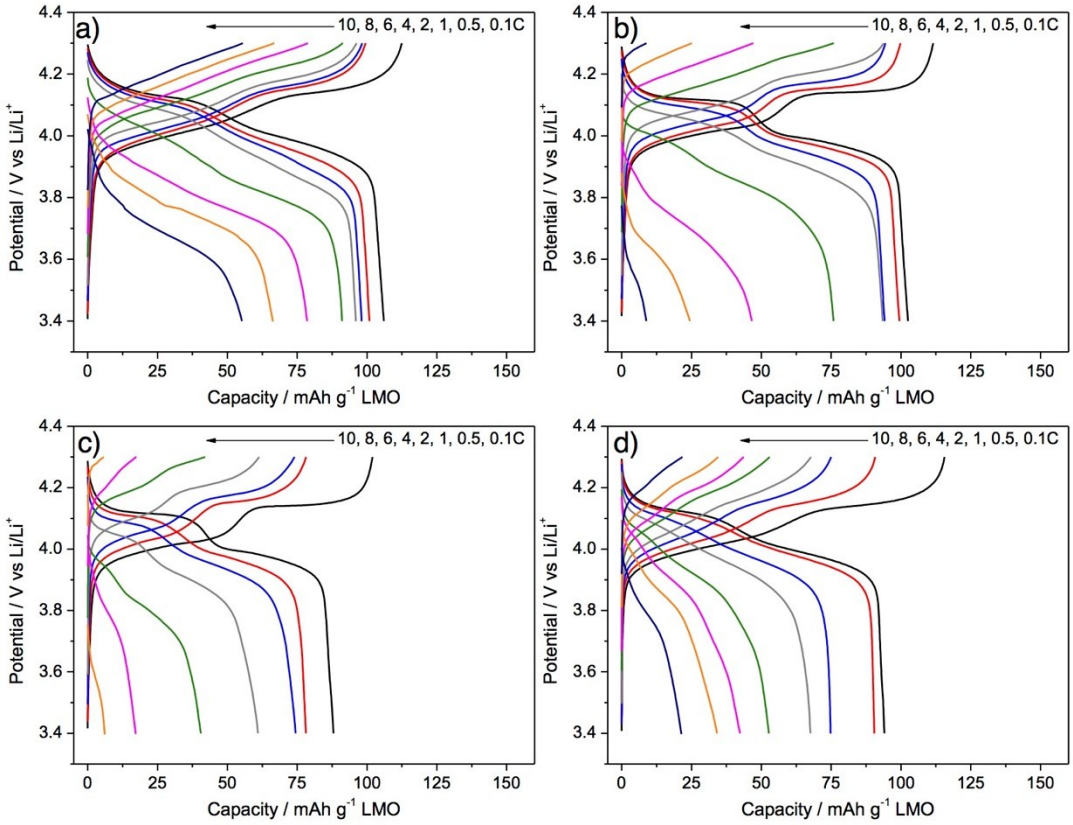

Fig. S9. Galvanostatic charge–discharge curves for a) LMO-350, b) LMO-500, c) LMO-700 and LMO-Comm at different C-rates.

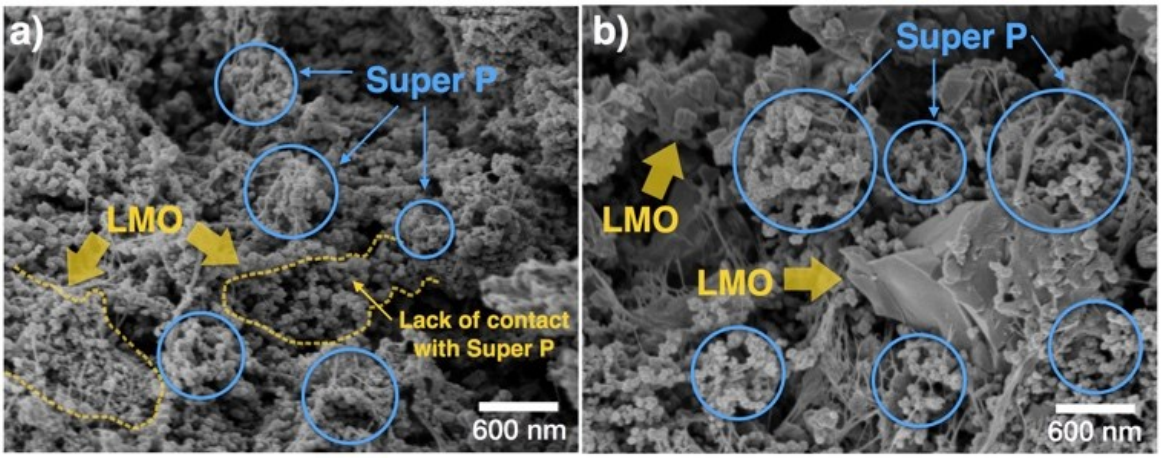

Fig. S10. Cross-sectional SEM images of a) LMO-500 electrode and b) LMO-Comm electrode. Domains rich in conductive carbon black are indicated by circles.

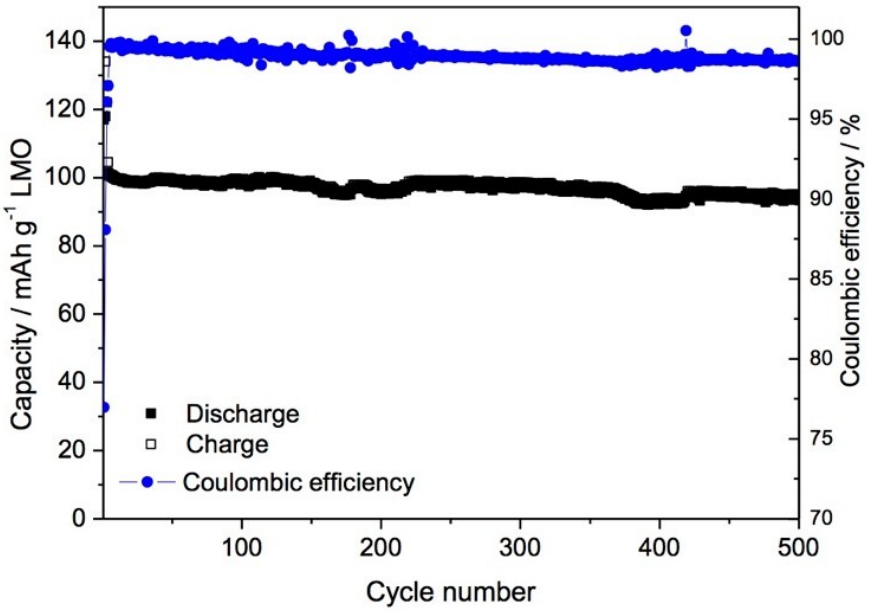

Fig. S11. Cyclic performance of LMO-HT at 4 C for 500 cycles. First 3 cycles were tested at C/10.

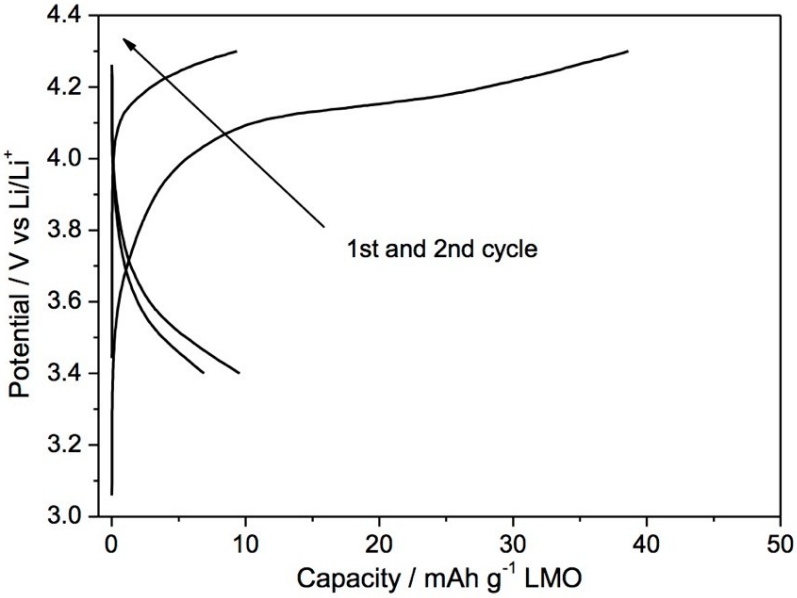

Fig. S12. Galvanostatic charge–discharge curves at 0.1 C for LMO-HT electrode formulated with Starbon® A800 (as alternative carbon additive) and PVDF. The weight ratio of LMO-HT : A800 : PVDF is 82 : 12 : 6.